

3. MODELING OF PARALLEL THREE-PHASE CURRENT-UNIDIRECTIONAL CONVERTERS

This chapter develops the models of the parallel three-phase current-unidirectional switch based converters, which include three-phase AC/DC buck rectifiers and DC/AC current source inverters.

3.1 TOPOLOGIES AND PARALLEL ARCHITECTURES

A three-phase buck rectifier and a three-phase current source inverter are shown in Figures 3.1 and 3.2, respectively. To simplify the discussion, the load for both converters is resistive.

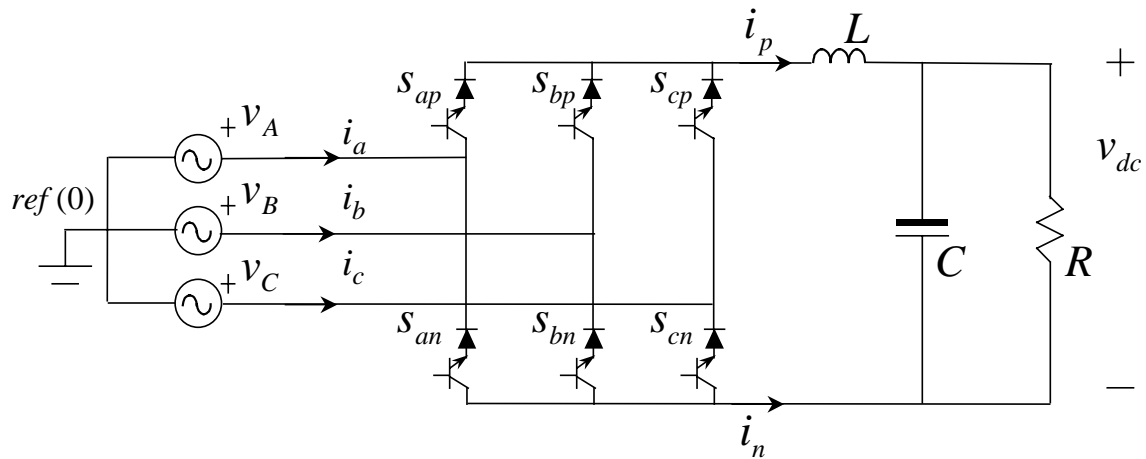


Figure 3.1 Three-phase buck rectifier.

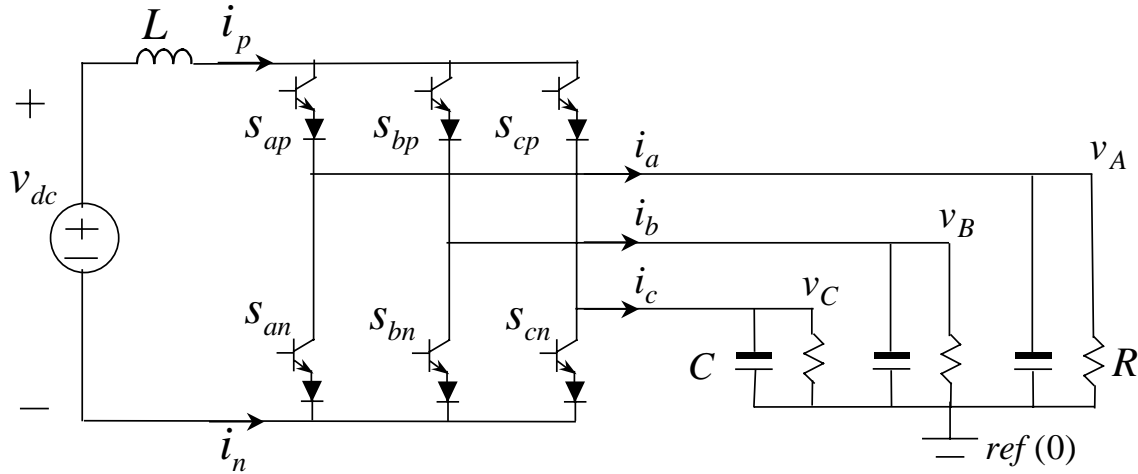


Figure 3.2 Three-phase current-source inverter.

Both buck rectifier and current source inverter are usually classified as current-unidirectional converters because they share the same switching cells that are current unidirectional. The switching cells either inherently have series diodes, for example, GTOs, or have external series blocking diodes. The symbolic representation and its voltage and current operational states are shown in Figure 3.3.

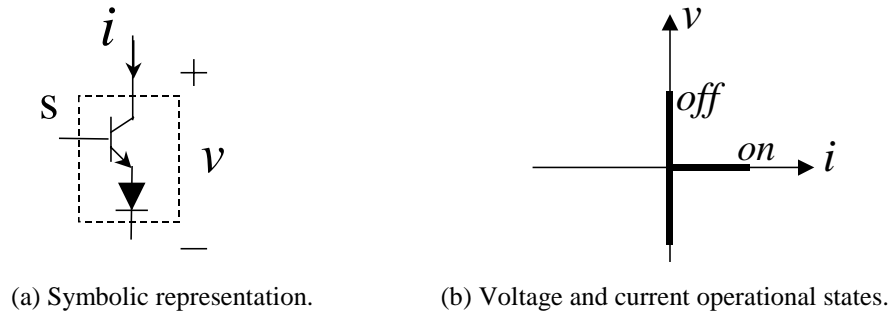


Figure 3.3 Current-unidirectional switching cell.

In this chapter, the average large-signal models and small-signal models of the parallel three-phase current-unidirectional converters are developed. Similar to the method used for the current-bidirectional converters, the current-unidirectional switching network is averaged on a rail arm basis. Conventionally, the averaging for a three-phase current-unidirectional converter is based on the average difference between the top and bottom switches in one phase leg [53]. This approach intentionally neglects common-mode components of the top and bottom DC rails. The common-mode components are generally of no interest in the control design for a single converter. However, they are

critical in the analysis and design of parallel converters. The rail-arm averaging adopts a reference point in the system, then derives the average values of all other points referring to the reference point. As a result, it allows the model to preserve the common-mode components. After the rail-arm averaging, the average model of a three-phase current-unidirectional converter can be easily obtained by connecting a top and bottom average rail arms.

For convenience, the reference point of the converter is chosen at the neutral point of the AC side of the circuit, as shown in Figures 3.1 and 3.2.

Figures 3.4 and 3.5 show the parallel buck rectifiers and current source inverters. Assuming the parallel converter systems double the power rating, then the output capacitance becomes $2C$, and the output resistance becomes $R/2$, where C and R are the parameters of a single converter in Figures 3.1 and 3.2.

In contrast to the single converter, the DC rail inductor in the parallel converters is split into two inductors at both top and bottom DC rails in order to avoid switching interactions between the parallel converters.

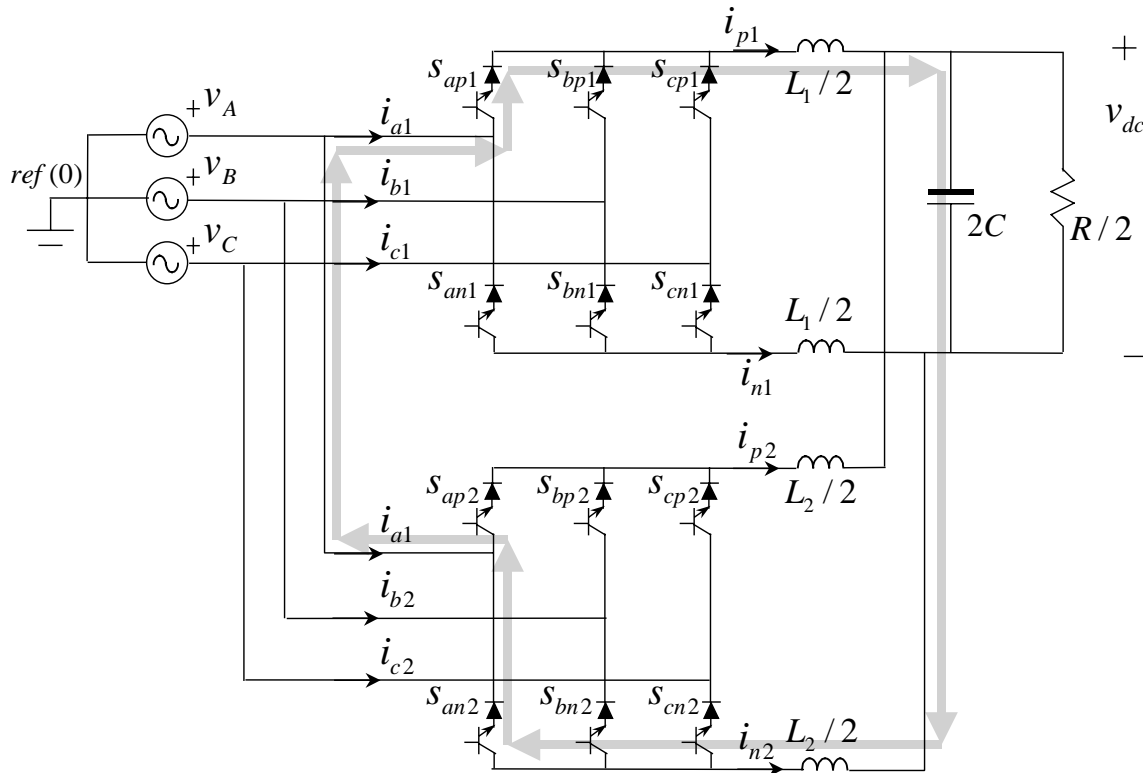


Figure 3.4 Circulating current in parallel three-phase buck rectifiers.

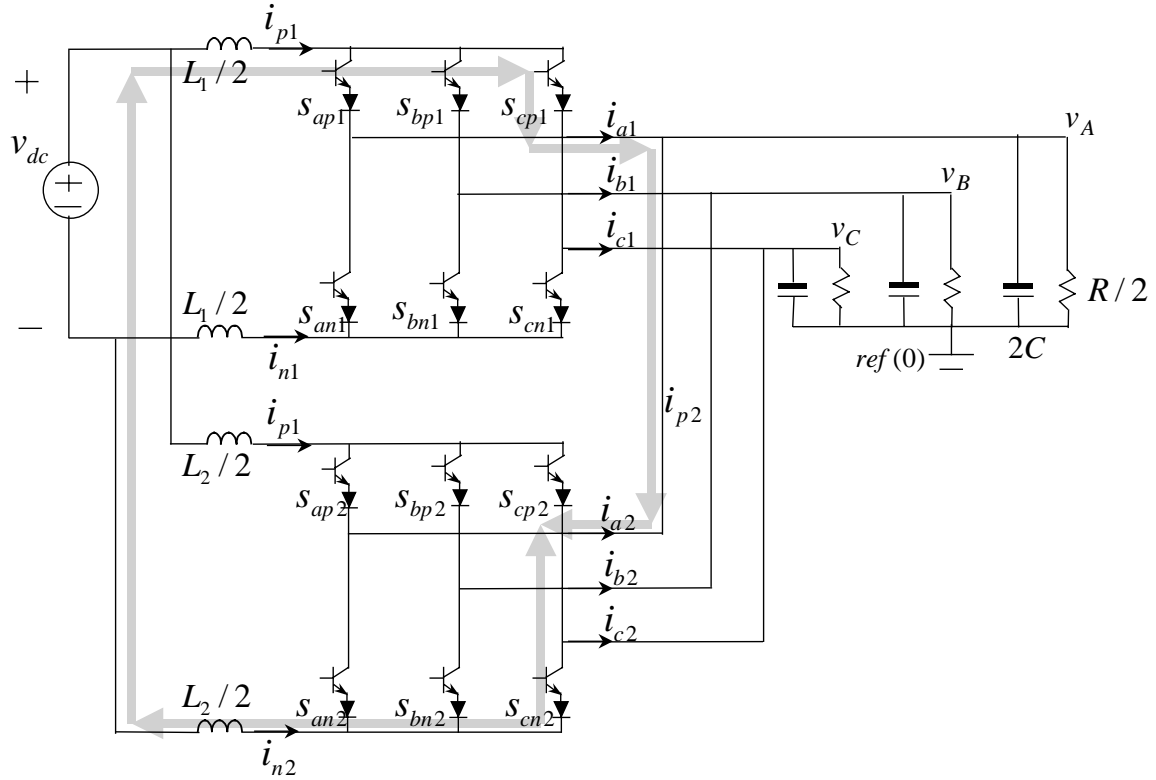


Figure 3.5 Circulating current in parallel three-phase current-source inverters.

Because of the direct paralleling, a circulating current exists, as highlighted in the Figures 3.4 and 3.5, for example. A zero-sequence current is defined, as in (2.1), in the parallel current-unidirectional converters.

3.2 AVERAGE MODELS

3.2.1 Rail-Arm Averaging

The switching cell in Figure 3.3(a) can be described by a generic switching s as in Figure 2.6. When s is open, that is, either the switch itself or the series diode blocks the voltage, referring to Figure 3.3(a), then the current i is zero. When s is closed, that is, both the switch and the series diode conduct a current, then the voltage v is zero. Therefore, a switching function s and the corresponding current and voltage values can be described as in (2.2).

In the current-unidirectional switch based converters, a generic switching unit, called a rail arm, can be identified, as shown in Figure 3.6. A rail arm is composed of three switching cells, and has voltage sources (or capacitors) on one side and a current source (or an inductor) on the other. These features make the rail arm a generic switching unit.

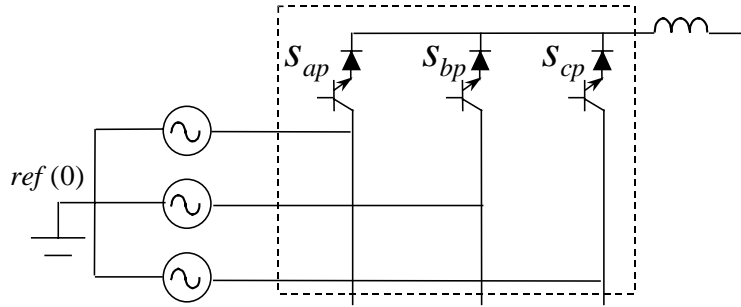


Figure 3.6 Top DC rail arm of current-unidirectional converters.

There are switching constrains for the three switching cells in the rail arm. To prevent the inductor from being open-circuited, one of the three switching cells, s_{ap} , s_{bp} or s_{cp} , has to be closed at any time. Meanwhile, to prevent the input voltage sources from being short-circuited, only one of the three switching cells can be closed at any time. This leads to the following relationship:

$$s_{ap} + s_{bp} + s_{cp} = 1. \quad (3.1)$$

Therefore, the rail arm can be represented by a single-pole, triple-throw switch, as shown in Figure 3.7. The input and output variables of interest are also defined in Figure 3.7.

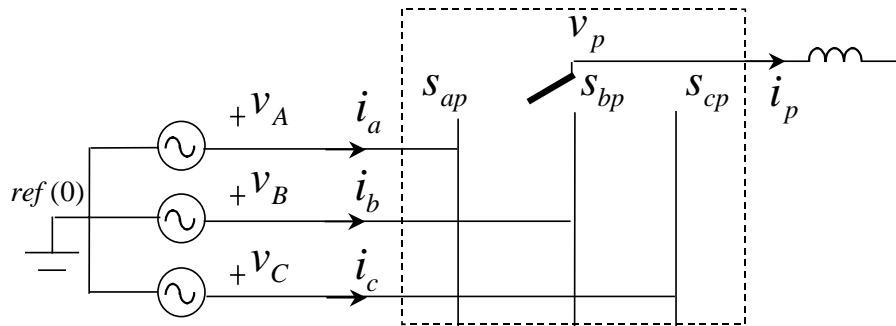


Figure 3.7 Top DC rail arm represented as a single-pole, triple-throw switch.

The PWM of the rail arm is shown in Figure 3.8, where T is the switching period, and d_{ap} , d_{bp} and d_{cp} are defined as the duty cycles of the switching cells s_{ap} , s_{bp} and s_{cp} ,

respectively. The corresponding voltage and current waveforms are also shown in Figure 3.8.

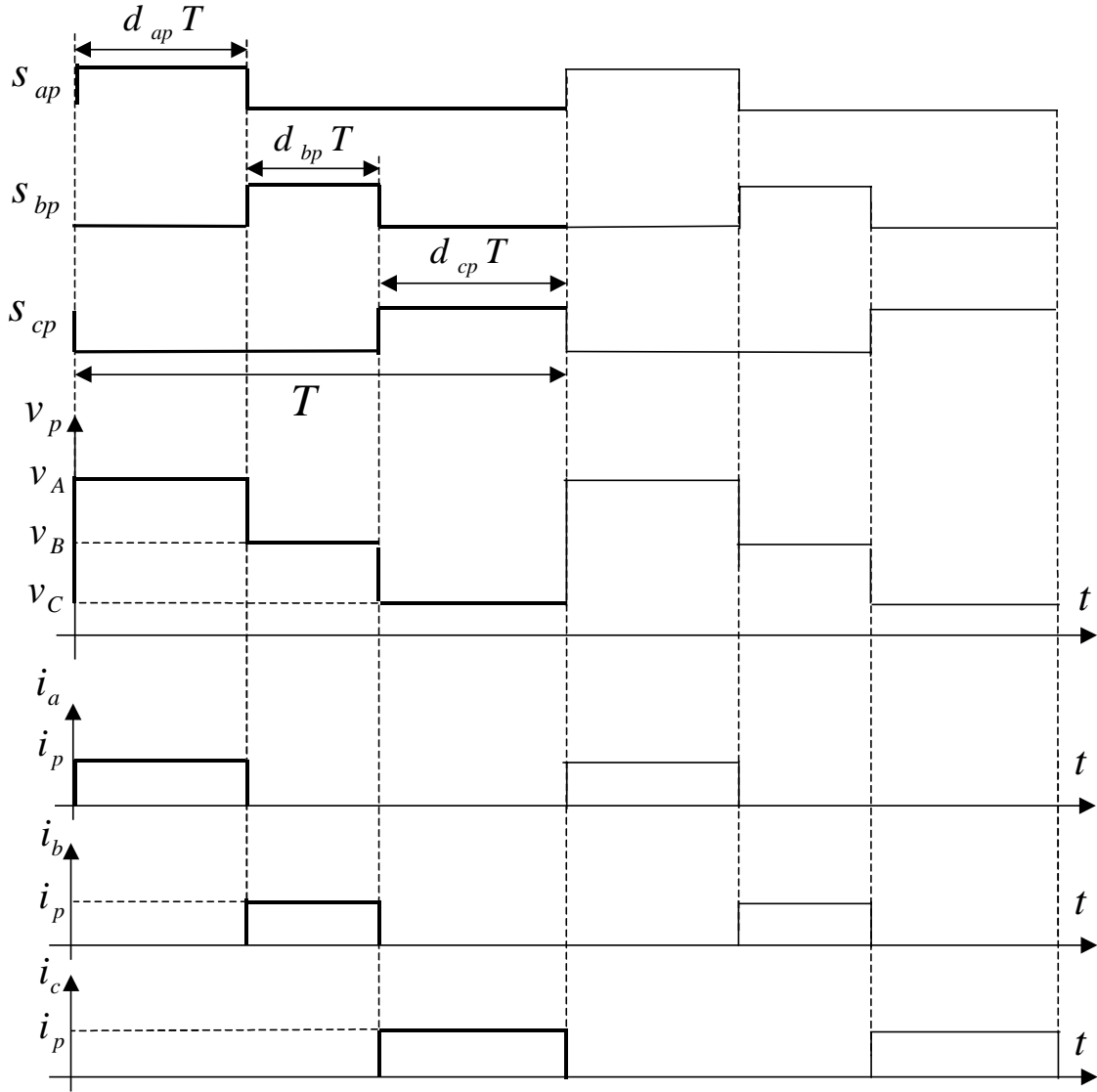


Figure 3.8 Rail arm PWM and corresponding current and voltage waveforms.

Based on the waveforms, one can obtain the voltage and current relationships in average, assuming the current i_p and the voltages v_A , v_B and v_C are continuous with small ripples:

$$v_p = \begin{bmatrix} d_{ap} & d_{bp} & d_{cp} \end{bmatrix} \cdot \begin{bmatrix} v_A \\ v_B \\ v_C \end{bmatrix}, \quad (3.2)$$

$$\begin{bmatrix} i_a \\ i_b \\ i_c \end{bmatrix} = \begin{bmatrix} d_{ap} \\ d_{bp} \\ d_{cp} \end{bmatrix} \cdot i_p . \quad (3.3)$$

$$d_{ap} + d_{bp} + d_{cp} = 1 . \quad (3.4)$$

The average model of the top rail arm is depicted in Figure 3.9. Equation (3.4) always holds due to the switching constraints of the rail arm.

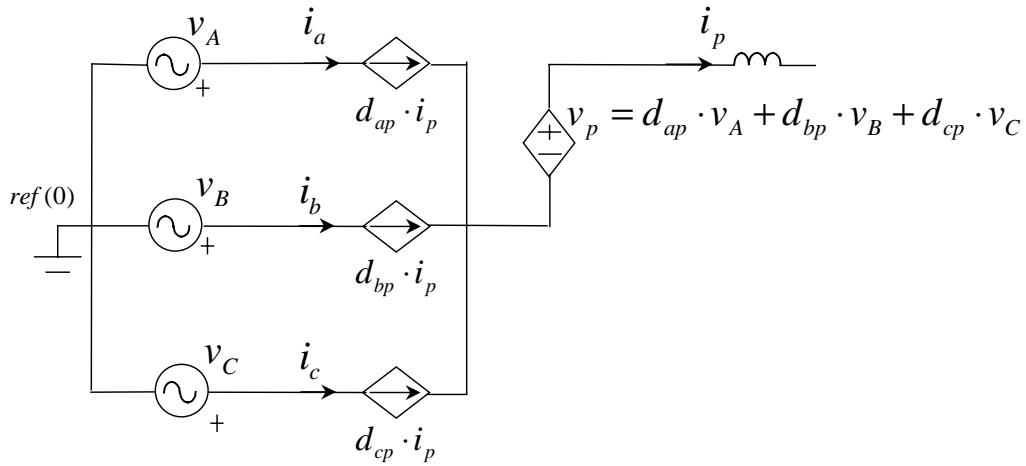


Figure 3.9 Top rail arm's average model.

A similar model can be developed for the bottom DC rail arm, shown in Figure 3.10.

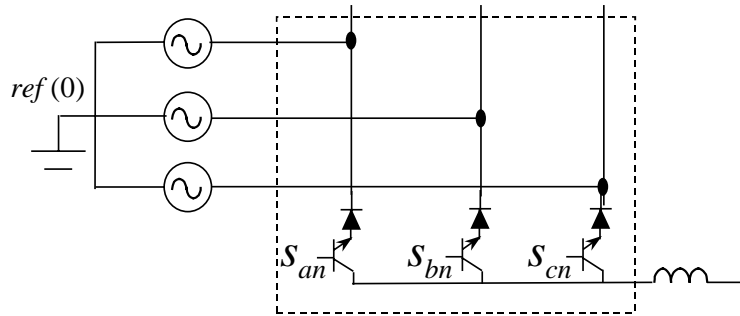


Figure 3.10 Bottom DC rail arm of current-unidirectional converters.

The average model of the bottom rail arm is shown in Figure 3.11.

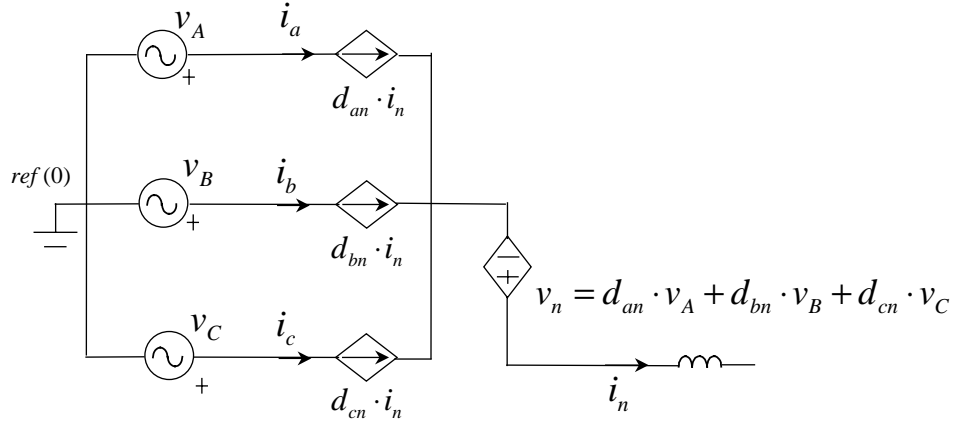


Figure 3.11 Bottom rail arm's average model.

where

$$v_n = \begin{bmatrix} d_{an} & d_{bn} & d_{cn} \end{bmatrix} \cdot \begin{bmatrix} v_A \\ v_B \\ v_C \end{bmatrix}, \quad (3.5)$$

$$\begin{bmatrix} i_a \\ i_b \\ i_c \end{bmatrix} = \begin{bmatrix} d_{an} \\ d_{bn} \\ d_{cn} \end{bmatrix} \cdot i_n, \quad (3.6)$$

$$d_{an} + d_{bn} + d_{cn} = 1. \quad (3.7)$$

Equation (3.7) always holds due the switching constraints of the rail arm. From Figures 3.10 and 3.11, it is obvious that the current i_n has a negative value because the actual current can only flow back into the AC side. However, the relationship between i_n and the phase currents still holds.

3.2.2 Average Model of Parallel Buck Rectifiers

After averaging the rail arms, the average model of a three-phase buck rectifier can be readily obtained by connecting the top and bottom rail arms as well as the rest of the circuit components. Figure 3.12 shows the average model of the buck rectifier, where

$$\begin{bmatrix} i_a \\ i_b \\ i_c \end{bmatrix} = \begin{bmatrix} d_{ap} \\ d_{bp} \\ d_{cp} \end{bmatrix} \cdot i_p + \begin{bmatrix} d_{an} \\ d_{bn} \\ d_{cn} \end{bmatrix} \cdot i_n. \quad (3.8)$$

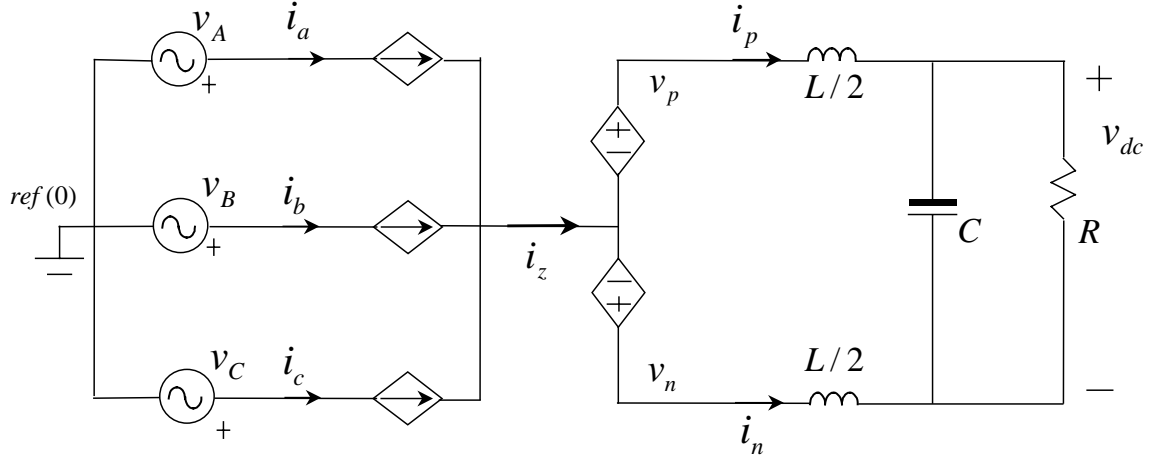


Figure 3.12 Buck rectifier's average model in stationary coordinates.

The state-space equations of the buck rectifier are:

$$\frac{di_p}{dt} = \frac{1}{L} \begin{bmatrix} d_{ap} - d_{an} & d_{bp} - d_{bn} & d_{cp} - d_{cn} \end{bmatrix} \cdot \begin{bmatrix} v_A \\ v_B \\ v_C \end{bmatrix} - \frac{1}{L} v_{dc}, \quad (3.9)$$

$$\frac{dv_{dc}}{dt} = \frac{1}{C} i_p - \frac{1}{RC} v_{dc}. \quad (3.10)$$

It can be seen from Figure 3.12 that, the zero-sequence current is always zero because physically there is no such current path. In parallel operation, however, a circulating current path is formed, as shown in Figure 3.13.

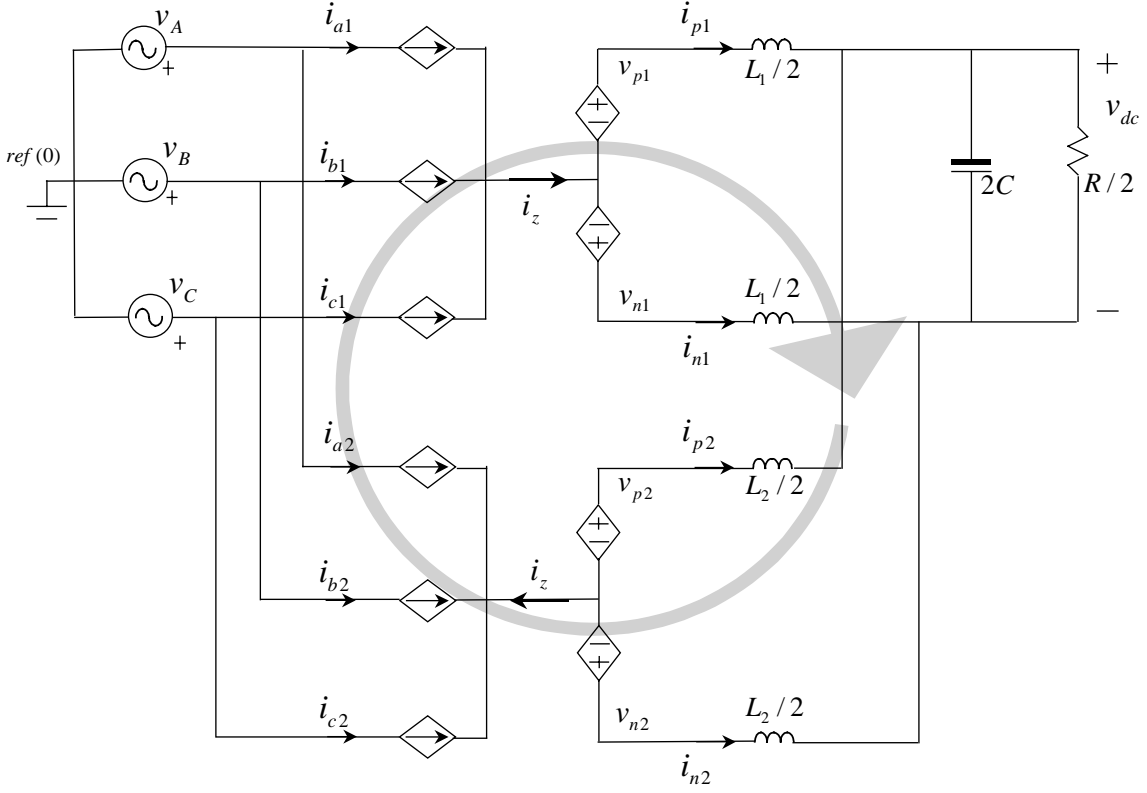


Figure 3.13 Parallel buck rectifiers' average model in stationary coordinates.

The state-space equations of the parallel buck rectifiers are:

$$v_{p1} - v_{n1} = \frac{L_1}{2} \frac{di_{p1}}{dt} + v_{dc} - \frac{L_1}{2} \frac{di_{n1}}{dt}, \quad (3.11)$$

$$v_{p2} - v_{n2} = \frac{L_2}{2} \frac{di_{p2}}{dt} + v_{dc} - \frac{L_2}{2} \frac{di_{n2}}{dt}, \quad (3.12)$$

$$v_{p1} - v_{p2} = \frac{L_1}{2} \frac{di_{p1}}{dt} - \frac{L_2}{2} \frac{di_{p2}}{dt}, \quad (3.13)$$

$$v_{n1} - v_{n2} = \frac{L_1}{2} \frac{di_{n1}}{dt} - \frac{L_2}{2} \frac{di_{n2}}{dt}, \quad (3.14)$$

$$\frac{dv_{dc}}{dt} = \frac{i_{p1} + i_{p2}}{2C} - \frac{v_{dc}}{RC}. \quad (3.15)$$

(3.11)-(3.14) can be simplified as

$$\frac{di_{p1}}{dt} = \frac{v_{pn1}}{L_1} - \frac{v_{dc}}{L_1} + \frac{\Delta v_z}{L_1 + L_2}, \quad (3.16)$$

$$\frac{di_{p2}}{dt} = \frac{v_{pn2}}{L_2} - \frac{v_{dc}}{L_2} - \frac{\Delta v_z}{L_1 + L_2}, \quad (3.17)$$

$$\frac{di_z}{dt} = \frac{2\Delta v_z}{L_1 + L_2}, \quad (3.18)$$

where i_z is defined as in (2.10), and

$$v_{pn1} = v_{p1} - v_{n1} = \begin{bmatrix} d_{ap1} - d_{an1} & d_{bp1} - d_{bn1} & d_{cp1} - d_{cn1} \end{bmatrix} \cdot \begin{bmatrix} v_A \\ v_B \\ v_C \end{bmatrix}, \quad (3.19)$$

$$v_{pn2} = v_{p2} - v_{n2} = \begin{bmatrix} d_{ap2} - d_{an2} & d_{bp2} - d_{bn2} & d_{cp2} - d_{cn2} \end{bmatrix} \cdot \begin{bmatrix} v_A \\ v_B \\ v_C \end{bmatrix}. \quad (3.20)$$

$$\Delta v_z = (v_{p1} + v_{n1}) - (v_{p2} + v_{n2}) = (v_{pn1} - v_{pn2}) - 2(v_{n1} - v_{n2}), \quad (3.21)$$

In steady state, the DC voltage v_{dc} is controlled as a constant value, while the phase currents i_{a1} , i_{b1} , i_{c1} , i_{a2} , i_{b2} and i_{c2} are controlled to be sinusoidal and in phase with the corresponding input phase voltages v_A , v_B and v_C , which are normally given as:

$$\begin{bmatrix} v_A \\ v_B \\ v_C \end{bmatrix} = \begin{bmatrix} V_m \cos(\omega t) \\ V_m \cos(\omega t - 2\pi/3) \\ V_m \cos(\omega t + 2\pi/3) \end{bmatrix}. \quad (3.22)$$

In order to have a DC steady state operating point (so as to linearize the system to design controllers), the model in stationary coordinates is usually transformed into rotating coordinates. The transformation matrix is chosen as in (2.15). The variables in the stationary coordinates can then be transformed into the rotating coordinates using (2.16).

Applying (2.16) to (3.9), one can obtain the average model of the buck rectifier in the rotating coordinates as described in (3.10) and (3.24):

$$\frac{di_p}{dt} = \frac{1}{L} \begin{bmatrix} d_d & d_q \end{bmatrix} \cdot \begin{bmatrix} v_d \\ v_q \end{bmatrix} - \frac{1}{L} v_{dc}. \quad (3.23)$$

where

$$\begin{bmatrix} d_d \\ d_q \\ 0 \end{bmatrix} = T \cdot \begin{bmatrix} d_{ap} - d_{an} \\ d_{bp} - d_{bn} \\ d_{cp} - d_{cn} \end{bmatrix}, \quad \begin{bmatrix} v_d \\ v_q \\ 0 \end{bmatrix} = T \cdot \begin{bmatrix} v_A \\ v_B \\ v_C \end{bmatrix} \quad (3.24)$$

Due to (3.4) and (3.7), the third row (d_z) is always zero. Therefore, it is dropped in (3.23).

Figure 3.14 shows the equivalent circuit of the model.

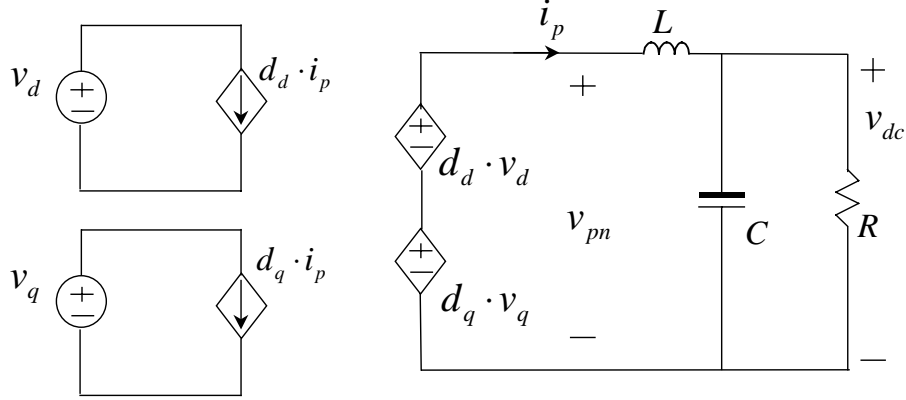


Figure 3.14 Buck rectifier's average model in rotating coordinates.

Applying (2.16) to (3.19)-(3.21), the average model of the parallel buck rectifiers in the rotating coordinates can be obtained as described in (3.15), (3-18) and (3-25)-(3-27):

$$\frac{di_{p1}}{dt} = \frac{1}{L_1} [d_{d1} \quad d_{q1}] \cdot \begin{bmatrix} v_d \\ v_q \end{bmatrix} - \frac{v_{dc}}{L_1} + \frac{\Delta v_z}{L_1 + L_2}, \quad (3.25)$$

$$\frac{di_{p2}}{dt} = \frac{1}{L_2} [d_{d2} \quad d_{q2}] \cdot \begin{bmatrix} v_d \\ v_q \end{bmatrix} - \frac{v_{dc}}{L_2} - \frac{\Delta v_z}{L_1 + L_2}, \quad (3.26)$$

$$\Delta v_z = [d_{d1} \quad d_{q1}] \cdot \begin{bmatrix} v_d \\ v_q \end{bmatrix} - [d_{d2} \quad d_{q2}] \cdot \begin{bmatrix} v_d \\ v_q \end{bmatrix} - 2([\Delta d_{dn} \quad \Delta d_{qn}] \cdot \begin{bmatrix} v_d \\ v_q \end{bmatrix}). \quad (3.27)$$

where:

$$\begin{bmatrix} d_{d1} \\ d_{q1} \\ 0 \end{bmatrix} = T \cdot \begin{bmatrix} d_{ap1} - d_{an1} \\ d_{bp1} - d_{bn1} \\ d_{cp1} - d_{cn1} \end{bmatrix}, \quad \begin{bmatrix} d_{d2} \\ d_{q2} \\ 0 \end{bmatrix} = T \cdot \begin{bmatrix} d_{ap2} - d_{an2} \\ d_{bp2} - d_{bn2} \\ d_{cp2} - d_{cn2} \end{bmatrix}, \quad \begin{bmatrix} \Delta d_{dn} \\ \Delta d_{qn} \\ 0 \end{bmatrix} = T \cdot \begin{bmatrix} d_{an1} - d_{an2} \\ d_{bn1} - d_{bn2} \\ d_{cn1} - d_{cn2} \end{bmatrix}. \quad (3.28)$$

The equivalent circuit of the model is shown in Figure 3.15. It is a fourth-order system with six control variables. It can be seen that a zero-sequence current is present in

the z channel. The current is determined by the difference between the two parallel converters' common-mode voltages.

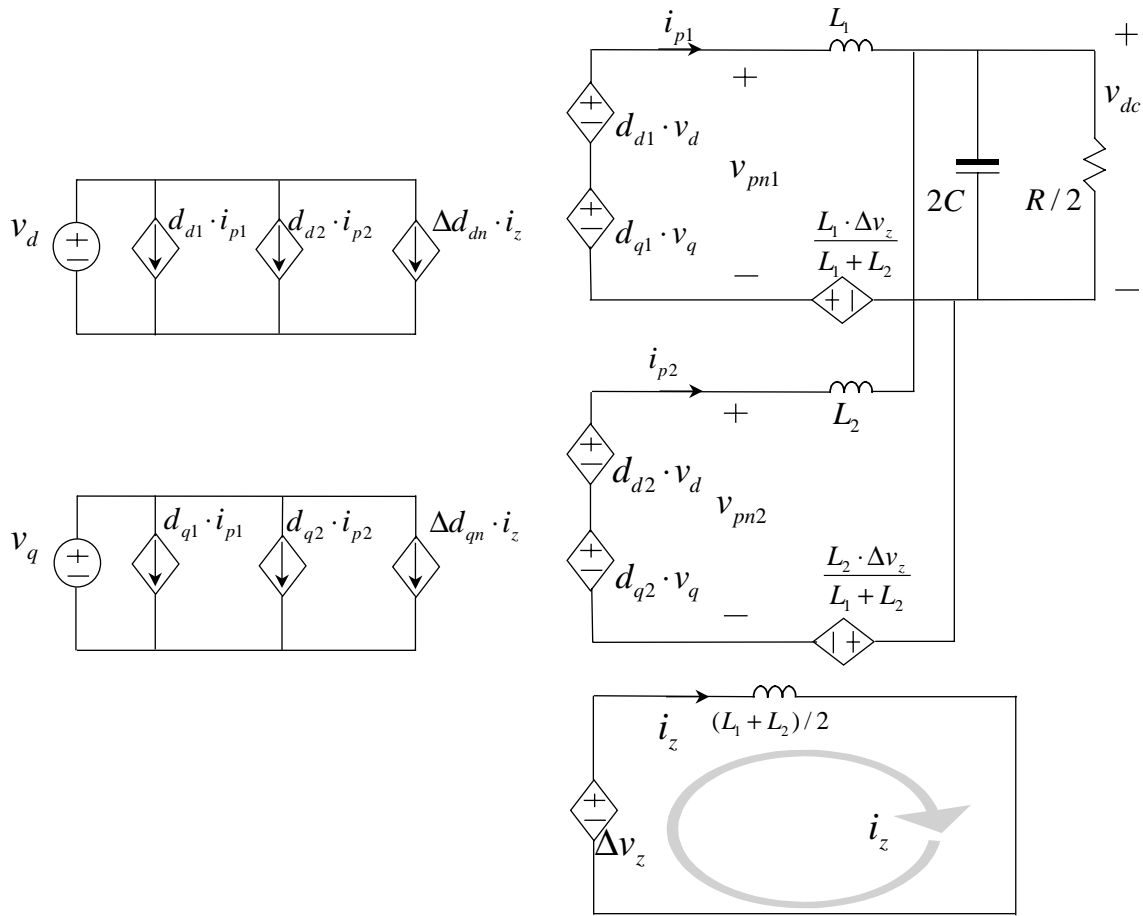


Figure 3.15 Parallel buck rectifiers' average model in rotating coordinates.

3.2.3 Average Model of Parallel Current Source Inverters

The average model of the current source inverter can be obtained by connecting the top and bottom rail arms as well as the rest of the circuit components, as shown in Figure 3.16.

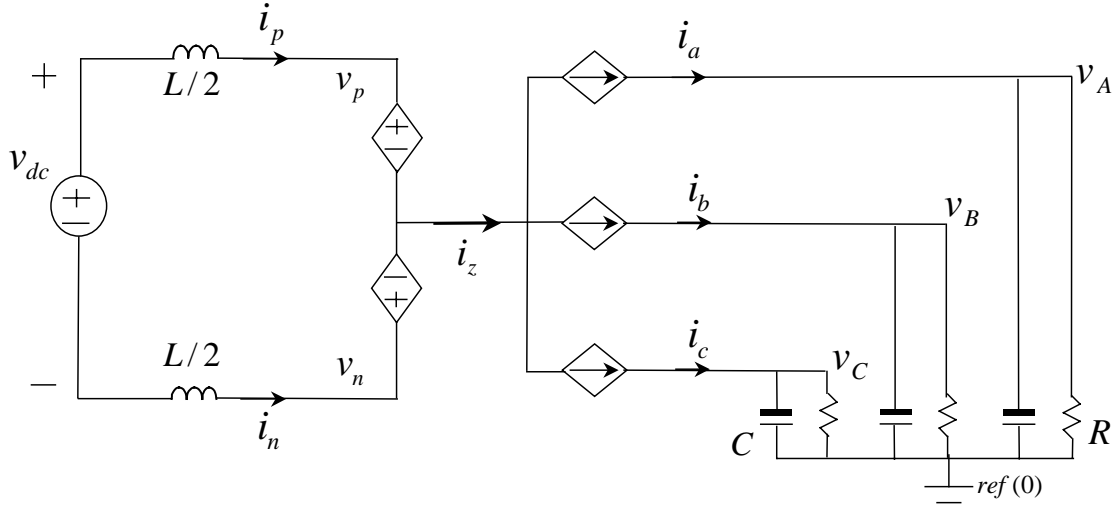


Figure 3.16 Current-source inverter's average model in stationary coordinates.

The state-space equations of the current source inverter are:

$$\frac{di_p}{dt} = \frac{1}{L}v_{dc} - \frac{1}{L} \begin{bmatrix} d_{ap} - d_{an} & d_{bp} - d_{bn} & d_{cp} - d_{cn} \end{bmatrix} \cdot \begin{bmatrix} v_A \\ v_B \\ v_C \end{bmatrix}, \quad (3.29)$$

$$\frac{d}{dt} \begin{bmatrix} v_A \\ v_B \\ v_C \end{bmatrix} = \frac{1}{C} \begin{bmatrix} d_{ap} - d_{an} \\ d_{bp} - d_{bn} \\ d_{cp} - d_{cn} \end{bmatrix} \cdot i_p - \frac{1}{R} \begin{bmatrix} v_A \\ v_B \\ v_C \end{bmatrix}. \quad (3.30)$$

As shown in Figure 3.16, the zero-sequence current is always zero because there is no such current path. Therefore, $i_n = -i_p$. In parallel operation, a circulating current path is formed, as shown in Figure 3.17.

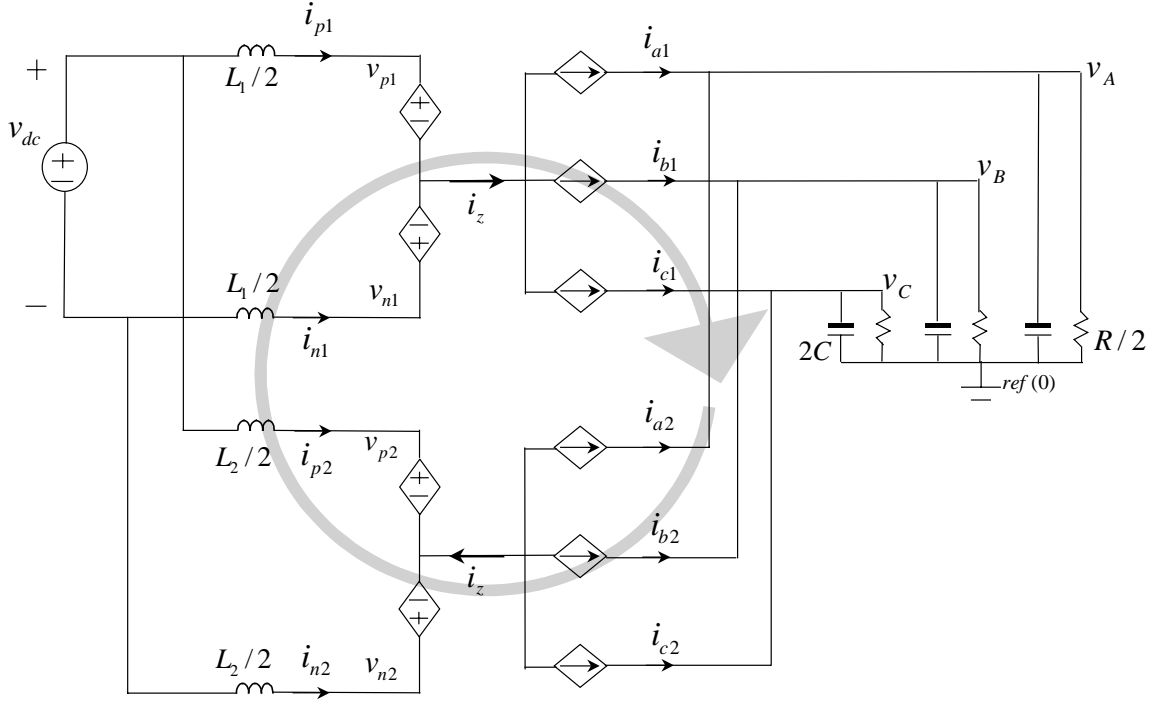


Figure 3.17 Parallel current-source inverters' average model in stationary coordinates.

The state-space equations of the parallel current source inverters are:

$$v_{dc} = v_{p1} - v_{n1} + \frac{L_1}{2} \frac{di_{p1}}{dt} - \frac{L_1}{2} \frac{di_{n1}}{dt}, \quad (3.31)$$

$$v_{dc} = v_{p2} - v_{n2} + \frac{L_2}{2} \frac{di_{p2}}{dt} - \frac{L_2}{2} \frac{di_{n2}}{dt}, \quad (3.32)$$

$$\begin{bmatrix} d_{ap1} \\ d_{bp1} \\ d_{cp1} \end{bmatrix} \cdot i_{p1} + \begin{bmatrix} d_{an1} \\ d_{bn1} \\ d_{cn1} \end{bmatrix} \cdot i_{n1} + \begin{bmatrix} d_{ap2} \\ d_{bp2} \\ d_{cp2} \end{bmatrix} \cdot i_{p2} + \begin{bmatrix} d_{an2} \\ d_{bn2} \\ d_{cn2} \end{bmatrix} \cdot i_{n2} = 2C \frac{d}{dt} \begin{bmatrix} v_A \\ v_B \\ v_C \end{bmatrix} + \frac{2}{R} \begin{bmatrix} v_A \\ v_B \\ v_C \end{bmatrix}, \quad (3.33)$$

$$v_{p1} - v_{p2} = -\frac{L_1}{2} \frac{di_{p1}}{dt} + \frac{L_2}{2} \frac{di_{p2}}{dt}, \quad (3.34)$$

$$v_{n1} - v_{n2} = -\frac{L_1}{2} \frac{di_{n1}}{dt} + \frac{L_2}{2} \frac{di_{n2}}{dt}. \quad (3.35)$$

Simplifying these equations, one can obtain:

$$\frac{di_{p1}}{dt} = \frac{v_{dc}}{L_1} - \frac{v_{pn1}}{L_1} - \frac{\Delta v_z}{L_1 + L_2}, \quad (3.36)$$

$$\frac{di_{p2}}{dt} = \frac{v_{dc}}{L_2} - \frac{v_{pn2}}{L_2} + \frac{\Delta v_z}{L_1 + L_2}, \quad (3.37)$$

$$\frac{di_z}{dt} = -\frac{2\Delta v_z}{L_1 + L_2}, \quad (3.38)$$

$$\frac{d}{dt} \begin{bmatrix} v_A \\ v_B \\ v_C \end{bmatrix} = \frac{1}{2C} \left(\begin{bmatrix} d_{ap1} - d_{an1} \\ d_{bp1} - d_{bn1} \\ d_{cp1} - d_{cn1} \end{bmatrix} \cdot i_{p1} + \begin{bmatrix} d_{ap2} - d_{an2} \\ d_{bp2} - d_{bn2} \\ d_{cp2} - d_{cn2} \end{bmatrix} \cdot i_{p2} + \begin{bmatrix} d_{an1} - d_{an2} \\ d_{bn1} - d_{bn2} \\ d_{cn1} - d_{cn2} \end{bmatrix} \cdot i_z \right) - \frac{1}{RC} \begin{bmatrix} v_A \\ v_B \\ v_C \end{bmatrix} \quad (3.39)$$

In order to have a DC steady state operating point (so as to linearize the system to design controllers), the models are usually transformed from the stationary into the rotating coordinates.

Similarly, applying (2.16) to (3.29)-(3.30), one can obtain the average model of the current source inverter in the rotating coordinates:

$$\frac{di_p}{dt} = \frac{1}{L} v_{dc} - \frac{1}{L} \begin{bmatrix} d_d & d_q \end{bmatrix} \cdot \begin{bmatrix} v_d \\ v_q \end{bmatrix}, \quad (3.40)$$

$$\frac{d}{dt} \begin{bmatrix} v_d \\ v_q \end{bmatrix} = \frac{i_p}{C} \begin{bmatrix} d_d \\ d_q \end{bmatrix} - \begin{bmatrix} \frac{1}{RC} & -\omega \\ \omega & \frac{1}{RC} \end{bmatrix} \cdot \begin{bmatrix} v_d \\ v_q \end{bmatrix}. \quad (3.41)$$

Figure 3.18 shows the equivalent circuit of the model.

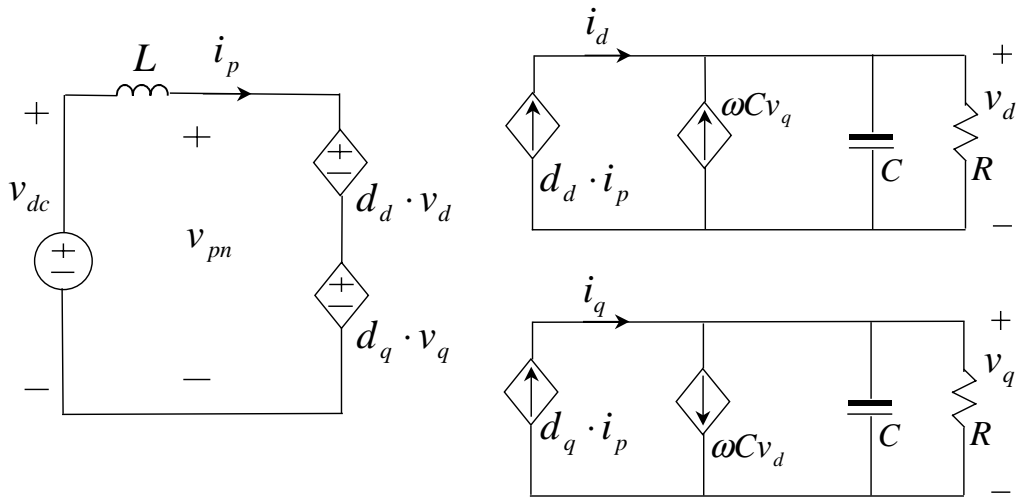


Figure 3.18 Current-source inverter's average model in rotating coordinates.

Applying (2.16) to (3.36)-(3.37) and (3-39), one can obtain the average model of the parallel current source inverters in the rotating coordinates, as described in (3.38), and (3.42)-(3.44):

$$\frac{di_{p1}}{dt} = \frac{v_{dc}}{L_1} - \frac{1}{L_1} \begin{bmatrix} d_{d1} & d_{q1} \end{bmatrix} \cdot \begin{bmatrix} v_d \\ v_q \end{bmatrix} - \frac{\Delta v_z}{L_1 + L_2}, \quad (3.42)$$

$$\frac{di_{p2}}{dt} = \frac{v_{dc}}{L_2} - \frac{1}{L_2} \begin{bmatrix} d_{d2} & d_{q2} \end{bmatrix} \cdot \begin{bmatrix} v_d \\ v_q \end{bmatrix} + \frac{\Delta v_z}{L_1 + L_2}, \quad (3.43)$$

$$\frac{d}{dt} \begin{bmatrix} v_d \\ v_q \end{bmatrix} = \frac{1}{2C} \begin{bmatrix} d_{d1} \\ d_{q1} \end{bmatrix} \cdot i_{p1} + \begin{bmatrix} d_{d2} \\ d_{q2} \end{bmatrix} \cdot i_{p2} + \begin{bmatrix} \Delta d_{dn} \\ \Delta d_{qn} \end{bmatrix} \cdot i_z - \begin{bmatrix} \frac{1}{RC} & -\omega \\ \omega & \frac{1}{RC} \end{bmatrix} \cdot \begin{bmatrix} v_d \\ v_q \end{bmatrix}. \quad (3.44)$$

The equivalent circuit of the model is shown in Figure 3.19.

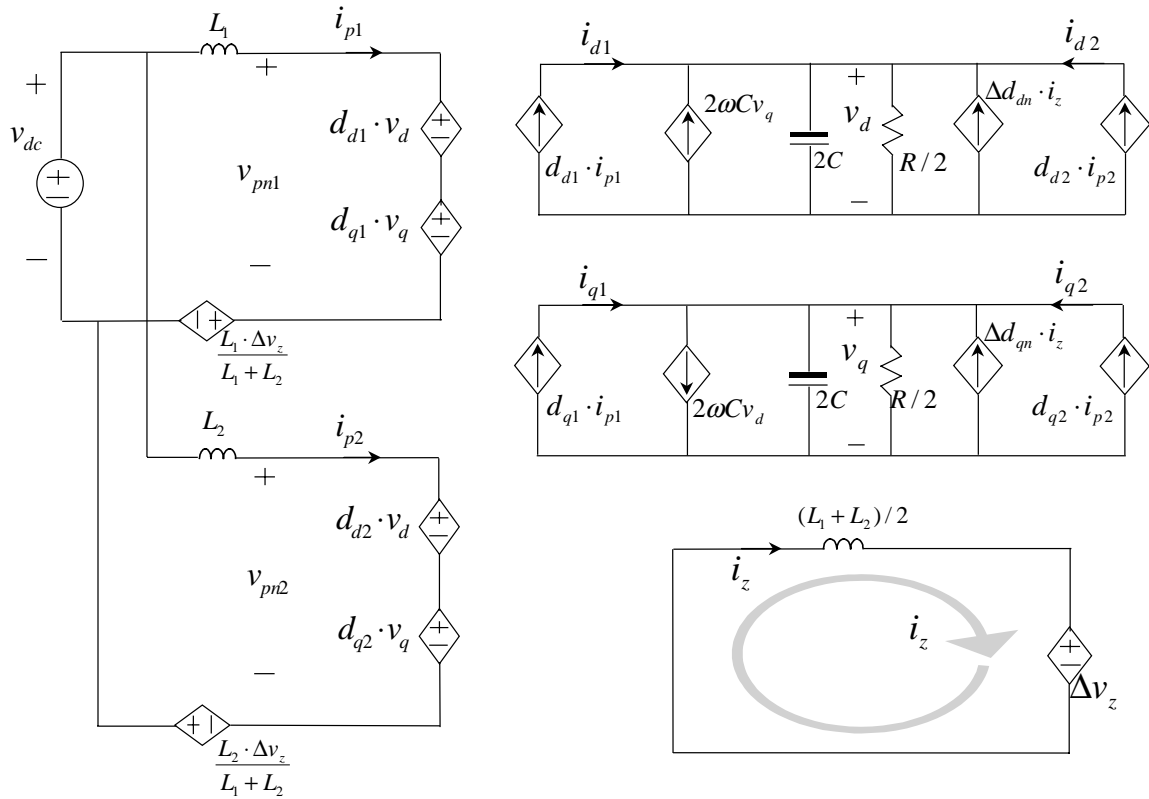


Figure 3.19 Parallel current-source inverters' average model in rotating coordinates.

3.3 SMALL-SIGNAL MODELS

3.3.1 Small-Signal Model of Parallel Buck Rectifiers

To obtain the small-signal model of the parallel three-phase buck rectifiers, a steady-state operating point is obtained first:

$$\begin{aligned}
 V_d &= \sqrt{\frac{3}{2}} \cdot V_m, & V_q &= 0, & V_z &= 0, \\
 D_{d1} = D_{d2} &= \frac{V_{dc}}{V_d}, & D_{q1} = D_{q2} &= 0, & \Delta D_{dn} = \Delta D_{qn} &= 0, \\
 I_{p1} = I_{p2} &= \frac{V_{dc}}{R}, & I_{q1} = I_{q2} &= 0, & I_z &= 0,
 \end{aligned} \tag{3.45}$$

where: R and V_m (given as in (3.22)) are given, V_{dc} , I_{q1} , I_{q2} and I_z are controlled to their reference values. I_{p1} , I_{p2} , D_{d1} , D_{d2} , D_{q1} , D_{q2} , ΔD_{dn} , ΔD_{qn} are calculated based on the given values and the control objectives.

Assuming that the input voltage sources are ideal, as in (2.48), then the small-signal model of the single buck rectifier is:

$$\frac{d}{dt} \begin{bmatrix} \tilde{v}_{dc} \\ \tilde{i}_p \end{bmatrix} = \begin{bmatrix} -\frac{1}{RC} & \frac{1}{C} \\ -\frac{1}{L} & 0 \end{bmatrix} \cdot \begin{bmatrix} \tilde{v}_{dc} \\ \tilde{i}_p \end{bmatrix} + \begin{bmatrix} 0 & 0 \\ \frac{V_d}{L} & \frac{V_q}{L} \end{bmatrix} \cdot \begin{bmatrix} \tilde{d}_d \\ \tilde{d}_q \end{bmatrix}. \tag{3.46}$$

The small-signal model of the parallel buck rectifiers can be derived as follows:

$$\frac{d}{dt} \begin{bmatrix} \tilde{v}_{dc} \\ \tilde{i}_{p1} \\ \tilde{i}_{p2} \\ \tilde{i}_z \end{bmatrix} = \begin{bmatrix} -\frac{1}{RC} & \frac{1}{2C} & \frac{1}{2C} & 0 \\ -\frac{1}{L_1} & 0 & 0 & 0 \\ -\frac{1}{L_2} & 0 & 0 & 0 \\ 0 & 0 & 0 & 0 \end{bmatrix} \cdot \begin{bmatrix} \tilde{v}_{dc} \\ \tilde{i}_{p1} \\ \tilde{i}_{p2} \\ \tilde{i}_z \end{bmatrix} + \begin{bmatrix} 0 & 0 & 0 & 0 & 0 \\ \frac{V_d}{L_1} & \frac{V_q}{L_1} & 0 & 0 & \frac{1}{L_1 + L_2} \\ 0 & 0 & \frac{V_d}{L_2} & \frac{V_q}{L_2} & \frac{-1}{L_1 + L_2} \\ 0 & 0 & 0 & 0 & \frac{2}{L_1 + L_2} \end{bmatrix} \cdot \begin{bmatrix} \tilde{d}_{d1} \\ \tilde{d}_{q1} \\ \tilde{d}_{d2} \\ \tilde{d}_{q2} \\ \Delta \tilde{v}_z \end{bmatrix} \tag{3.47}$$

The equivalent circuit is shown in Figure 3.20. Some terms are omitted because $I_z = 0$, $\Delta D_{dn} = 0$ and $\Delta D_{qn} = 0$ provided that the zero-sequence current is controlled to be zero.

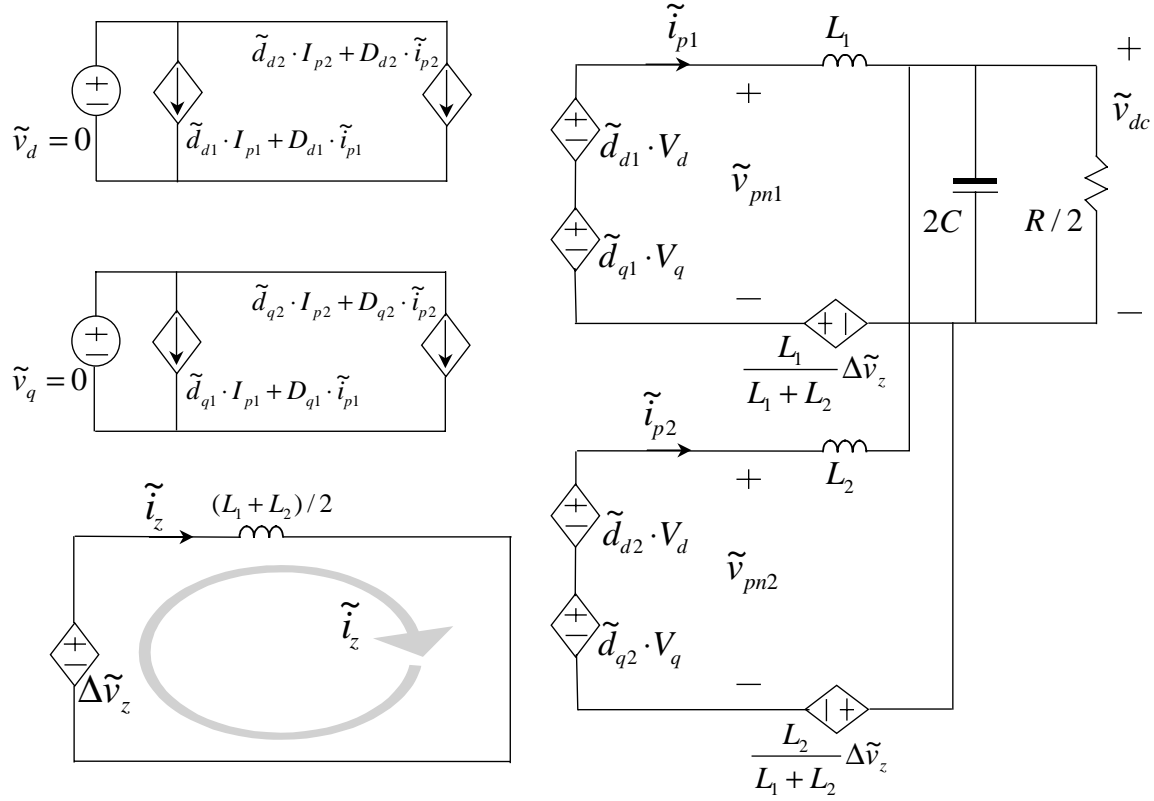


Figure 3.20 Parallel buck rectifiers' small-signal model.

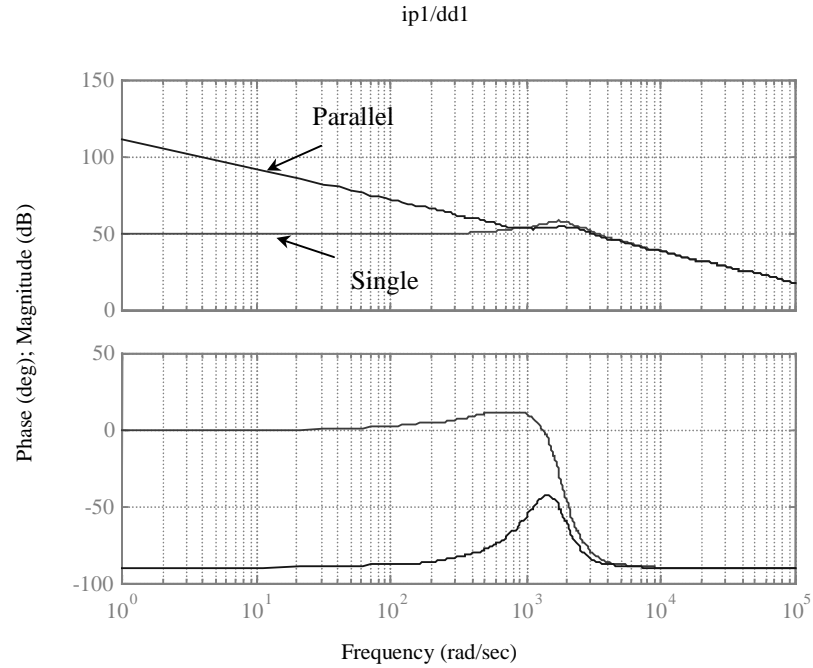
Unlike the model of the parallel boost rectifiers, the small-signal model of the parallel buck rectifiers shows that the z channel is not independent and is coupled with the DC side.

The open-loop transfer functions are simulated using MATLAB based on the parameters given below:

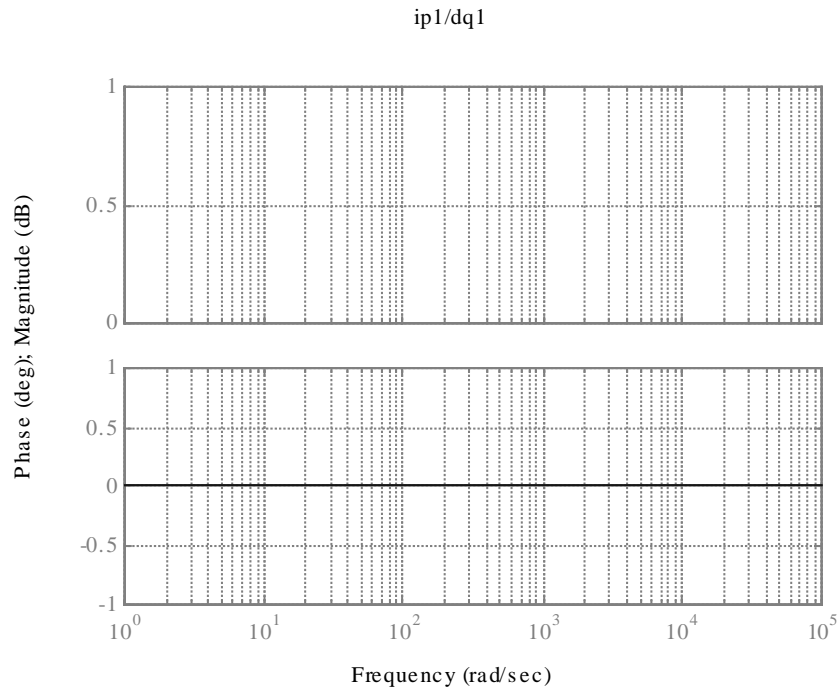
$$V_m = 120 \cdot \sqrt{2} \text{ V}; \quad \omega = 2\pi \cdot 60 \text{ rad/s}; \quad V_{dc} = 100 \text{ V}; \quad P_o = 15 \text{ kW}; \quad R = V_{dc}^2 / P_o;$$

$$L = 250 \mu\text{H}; \quad C = 1200 \mu\text{F}. \text{ Be noted that the parallel converter operation has } 2C \text{ and } R/2.$$

Figure 3.21(a) shows that, due to the zero-sequence interaction, the transfer function of d channel control to DC rail current in the parallel converters has a pole at the DC origin. With the inductor at the DC side, the transfer function does not have a double pole at rotating frequency as in the parallel boost rectifiers. Figure 3.21(b) shows that the q-channel control has no small-signal effect on the DC rail current. Figure 3.22 shows that the d- and q-channel controls have no small-signal effect on z-channel current. Figure 3.23 shows that the z-channel control has small-signal effect on both z-channel and DC output currents. Figure 3.24 shows that the two converters are cross-coupled.

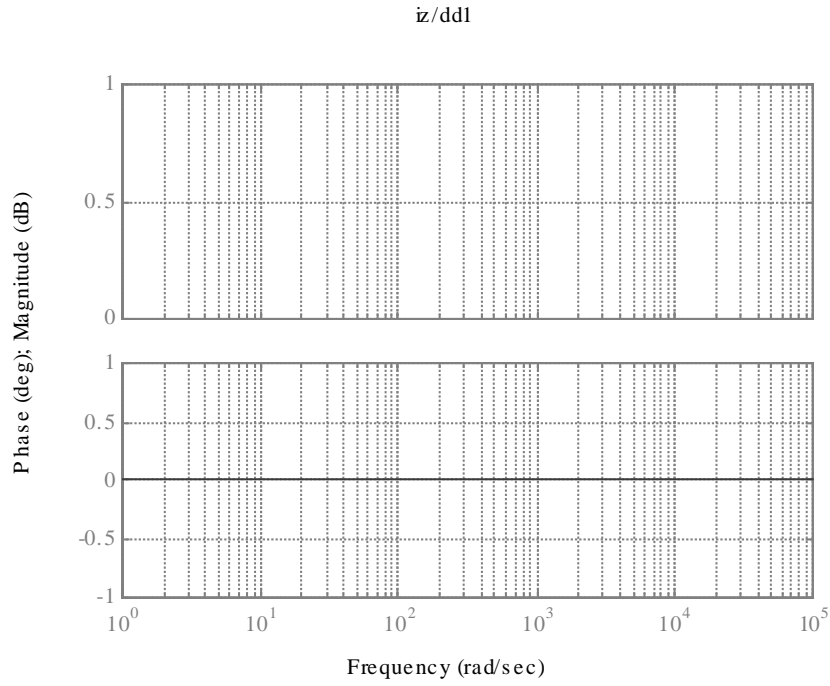


(a) $\tilde{i}_p / \tilde{d}_d$ (single) and $\tilde{i}_{p1} / \tilde{d}_{d1}$ (parallel).

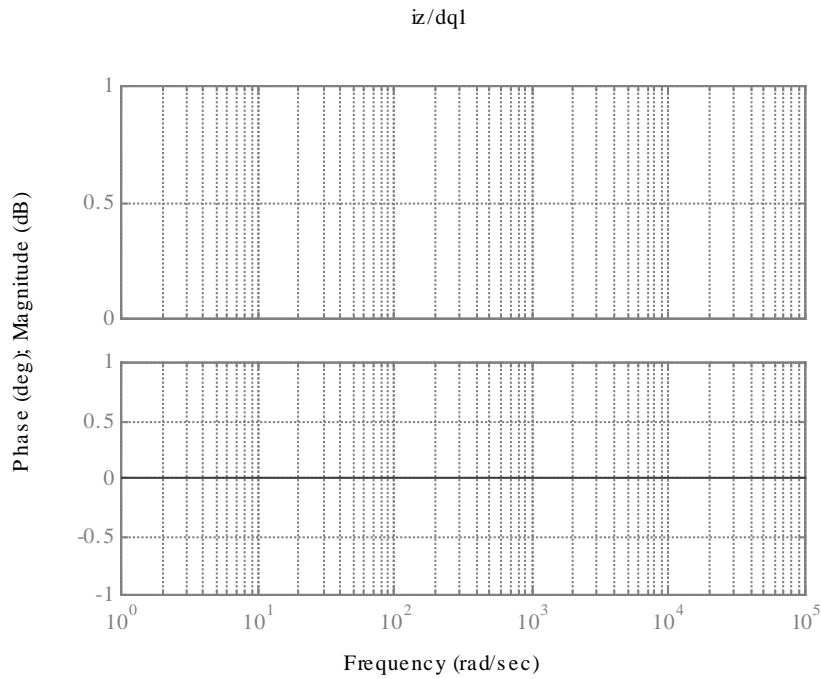


(b) $\tilde{i}_p / \tilde{d}_q$ (single) and $\tilde{i}_{p1} / \tilde{d}_{q1}$ (parallel).

Figure 3.21 Open-loop transfer functions of d- and q-channel control to DC output current.

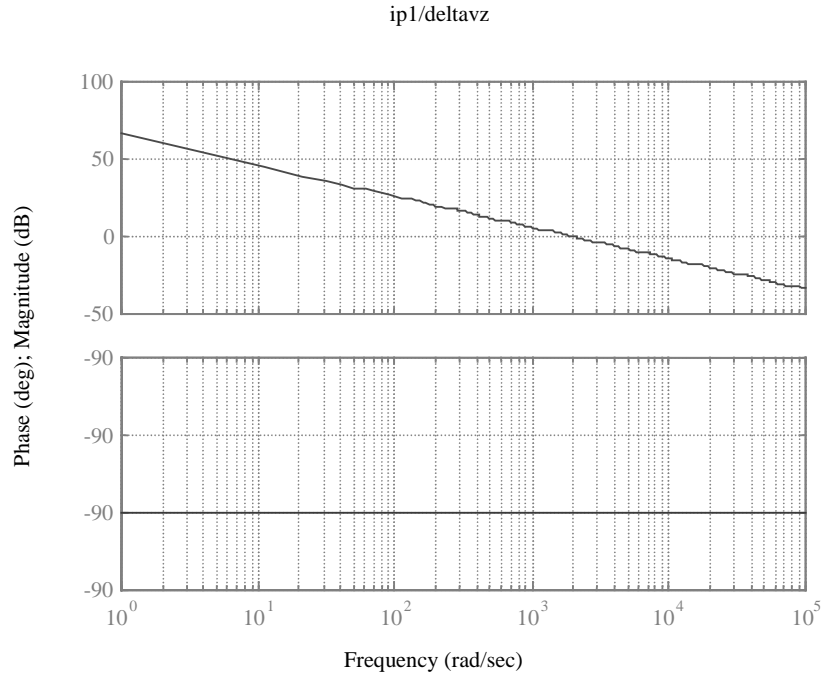


(a) $\tilde{i}_z / \tilde{d}_{d1}$.

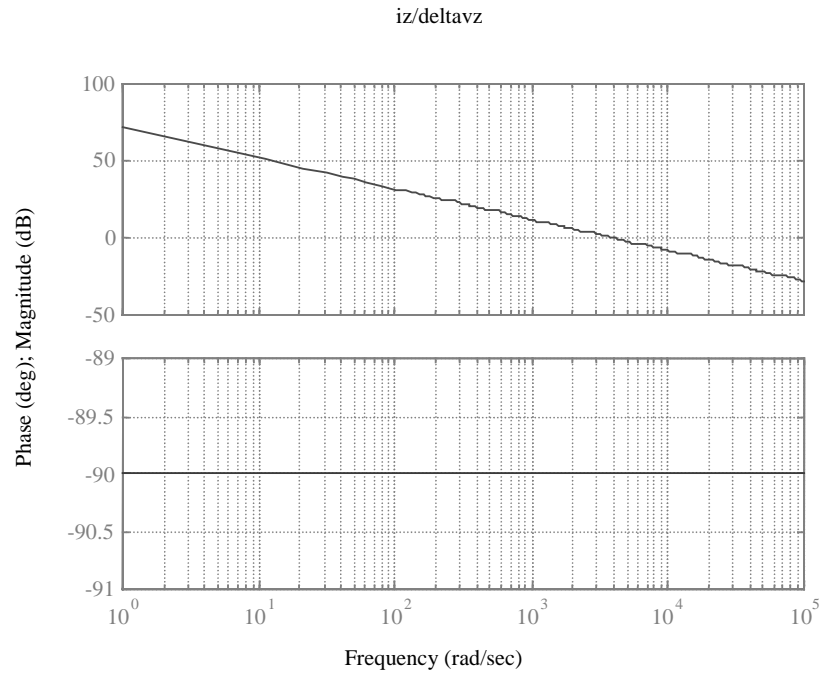


(b) $\tilde{i}_z / \tilde{d}_{q1}$.

Figure 3.22 Open-loop transfer functions of d- and q-channel control to z-channel current.



(a) $\tilde{i}_{p1} / \Delta\tilde{v}_z$.



(b) $\tilde{i}_z / \Delta\tilde{v}_z$.

Figure 3.23 Open-loop transfer functions of z-channel control to DC output and z-channel currents.

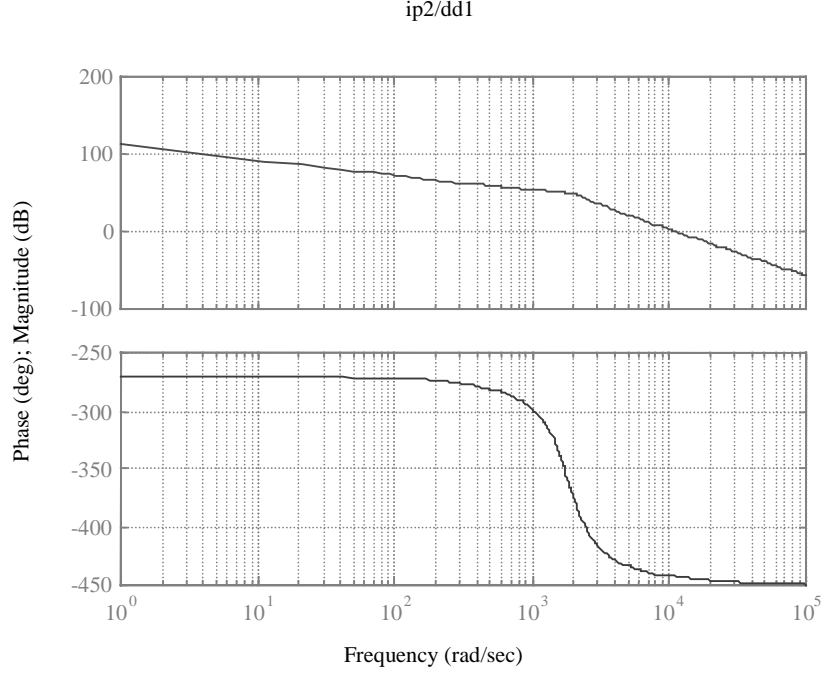


Figure 3.24 Open-loop transfer function $\tilde{i}_{p2} / \tilde{d}_{d1}$ shows the two converters are cross-coupled.

3.3.2 Small-Signal Model of Parallel Current Source Inverters

To obtain the small-signal model of the parallel three-phase current source inverter, a steady-state operating point is obtained as follows:

$$\begin{aligned}
 V_d &= \sqrt{\frac{3}{2}} \cdot V_m, & V_q &= 0, & I_{q1} &= I_{q2} = 0, & I_z &= 0 \\
 D_{d1} &= D_{d2} = \frac{V_{dc}}{V_d}, & D_{q1} &= D_{q2} = \frac{\omega C V_d}{I_{p1}}, & \Delta D_{dn} &= \Delta D_{qn} = 0, \\
 I_{p1} &= \frac{V_{dc}}{R D_{d1}}, & I_{p2} &= \frac{V_{dc}}{R D_{d2}}, & I_{d1} &= D_{d1} \cdot I_{p1}, & I_{d2} &= D_{d2} \cdot I_{p2},
 \end{aligned} \tag{3.48}$$

where: R , C and V_{dc} are given, V_d and V_q are so controlled that the transformed voltages are as in (3.22). I_{q1} , I_{q2} and I_z are controlled to their reference values. I_{p1} , I_{p2} , I_{d1} , I_{d2} , D_{d1} , D_{d2} , D_{q1} , D_{q2} , ΔD_{dn} , ΔD_{qn} are calculated based on the given values and the control objectives.

Assuming that the input voltage source is ideal, as in (2.52), then the small-signal model of the single current source inverter is:

$$\frac{d}{dt} \begin{bmatrix} \tilde{v}_d \\ \tilde{v}_q \\ \tilde{i}_p \end{bmatrix} = \begin{bmatrix} \frac{-1}{RC} & \omega & \frac{D_d}{C} \\ -\omega & \frac{-1}{RC} & \frac{D_q}{C} \\ -\frac{D_d}{L} & -\frac{D_q}{L} & 0 \end{bmatrix} \cdot \begin{bmatrix} \tilde{v}_d \\ \tilde{v}_q \\ \tilde{i}_p \end{bmatrix} + \begin{bmatrix} \frac{I_p}{C} & 0 \\ 0 & \frac{I_p}{C} \\ -\frac{V_d}{L} & -\frac{V_q}{L} \end{bmatrix} \cdot \begin{bmatrix} \tilde{d}_d \\ \tilde{d}_q \end{bmatrix}. \quad (3.49)$$

The small-signal model of the parallel current source inverters can be derived as follows:

$$\frac{d}{dt} \begin{bmatrix} \tilde{v}_d \\ \tilde{v}_q \\ \tilde{i}_{p1} \\ \tilde{i}_{p2} \\ \tilde{i}_z \end{bmatrix} = \begin{bmatrix} \frac{-1}{RC} & \omega & \frac{D_{d1}}{2C} & \frac{D_{d2}}{2C} & 0 \\ -\omega & \frac{-1}{RC} & \frac{D_{q1}}{2C} & \frac{D_{q2}}{2C} & 0 \\ -\frac{D_{d1}}{L_1} & -\frac{D_{q1}}{L_1} & 0 & 0 & 0 \\ -\frac{D_{d2}}{L_2} & -\frac{D_{q2}}{L_2} & 0 & 0 & 0 \\ 0 & 0 & 0 & 0 & 0 \end{bmatrix} \cdot \begin{bmatrix} \tilde{v}_d \\ \tilde{v}_q \\ \tilde{i}_{p1} \\ \tilde{i}_{p2} \\ \tilde{i}_z \end{bmatrix} + \begin{bmatrix} \frac{I_{p1}}{2C} & 0 & \frac{I_{p2}}{2C} & 0 & 0 \\ 0 & \frac{I_{p1}}{2C} & 0 & \frac{I_{p1}}{2C} & 0 \\ -\frac{V_d}{L_1} & -\frac{V_q}{L_1} & 0 & 0 & \frac{-1}{L_1+L_2} \\ 0 & 0 & -\frac{V_d}{L_2} & -\frac{V_q}{L_2} & \frac{1}{L_1+L_2} \\ 0 & 0 & 0 & 0 & \frac{-2}{L_1+L_2} \end{bmatrix} \cdot \begin{bmatrix} \tilde{d}_{d1} \\ \tilde{d}_{d2} \\ \tilde{d}_{q1} \\ \tilde{d}_{q2} \\ \Delta \tilde{v}_z \end{bmatrix}. \quad (3.50)$$

In the model, Δv_z is the control variable of z channel.

The equivalent circuit is shown in Figure 3.25.

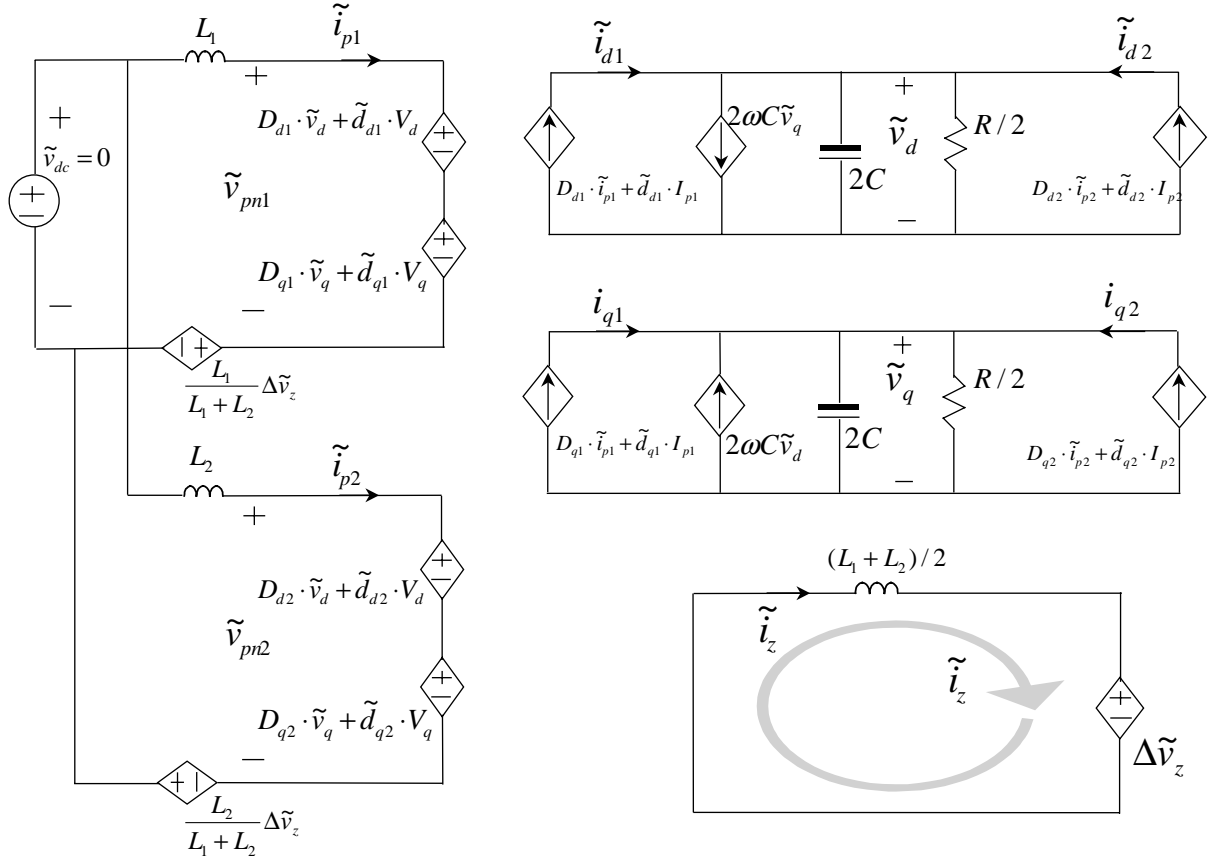
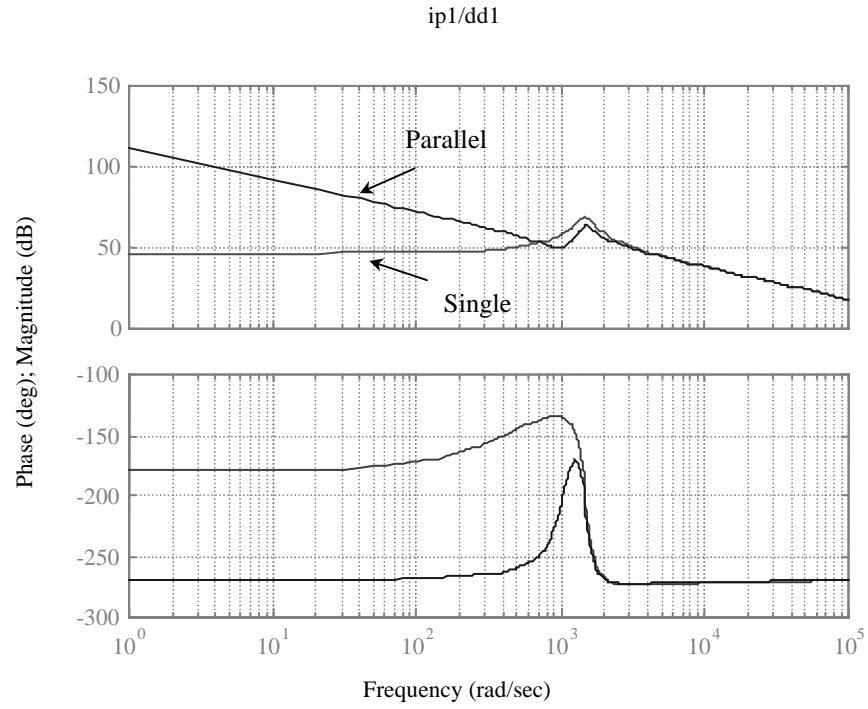


Figure 3.25 Parallel current-source inverters' small-signal model.

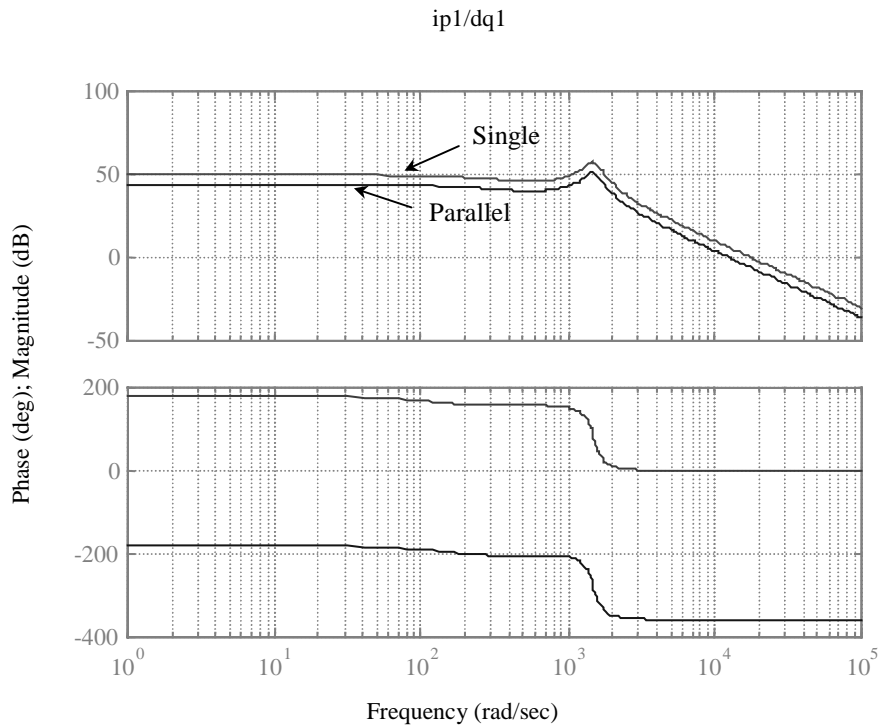
The open-loop transfer functions are simulated using MATLAB based on the parameters given below:

$V_m = 120 \cdot \sqrt{2}$ V; $\omega = 2\pi \cdot 60$ rad/s; $V_{dc} = 100$ V; $P_o = 15$ kW; $R = V_{dc}^2 / P_o$;
 $L = 250 \mu\text{H}$; $C = 1200 \mu\text{F}$. Be noted that the parallel converter operation has $2C$ and $R/2$.

Figure 3.26(a) shows that, due to the zero-sequence interaction, the transfer function of d-channel control to DC rail current in the parallel converters has a pole at the DC origin. Figure 3.26(b) shows that the q channel control, however, has no pole at the DC origin. Figure 3.27 shows that the d- and q-channel controls have no small-signal effect on z-channel current due to $V_q = 0$. Figure 3.28 shows that the z-channel control has small-signal effect on both z-channel and DC output currents. Figure 3.29 shows that the two converters are cross-coupled.

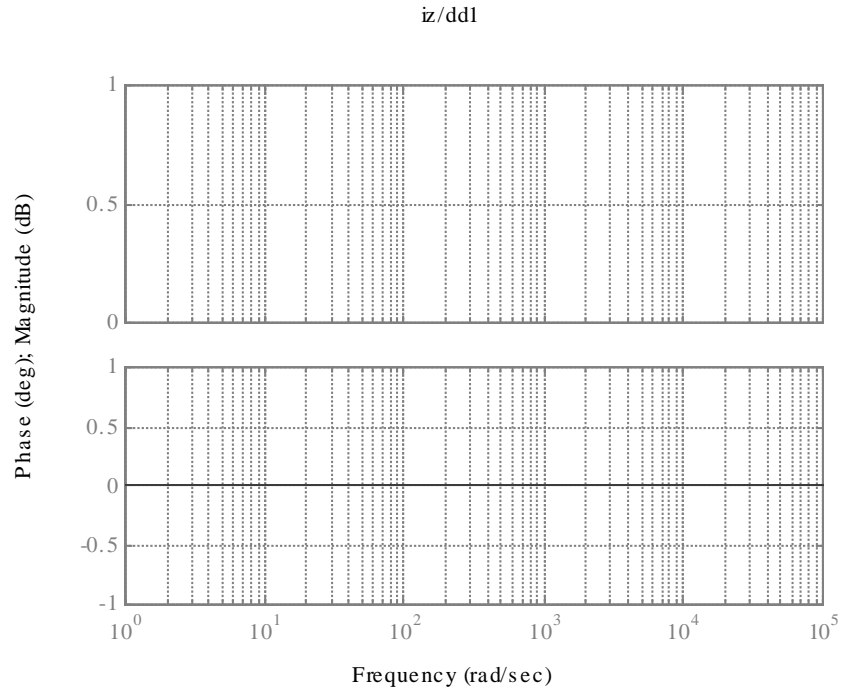


(a) $\tilde{i}_p / \tilde{d}_d$ (single) and $\tilde{i}_{p1} / \tilde{d}_{d1}$ (parallel).

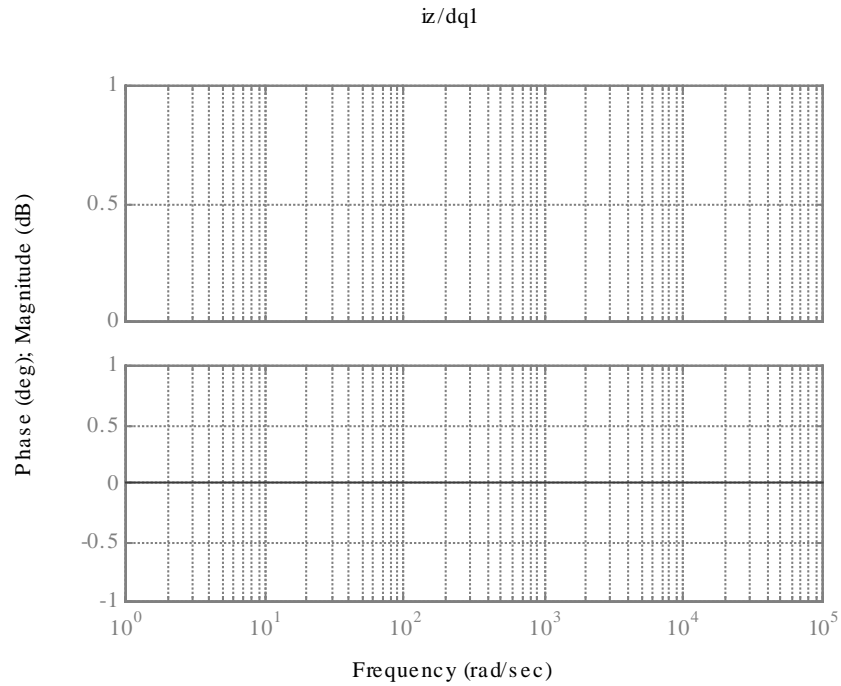


(b) $\tilde{i}_p / \tilde{d}_q$ (single) and $\tilde{i}_{p1} / \tilde{d}_{q1}$ (parallel).

Figure 3.26 Open-loop transfer functions of d- and q-channel control to DC output current.

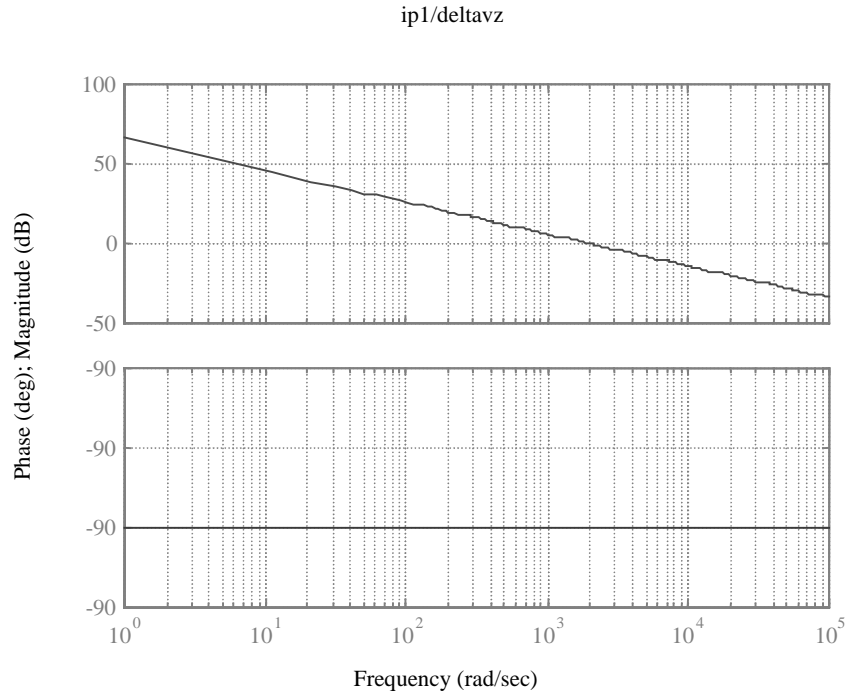


(a) $\tilde{i}_z / \tilde{d}_{d1}$.

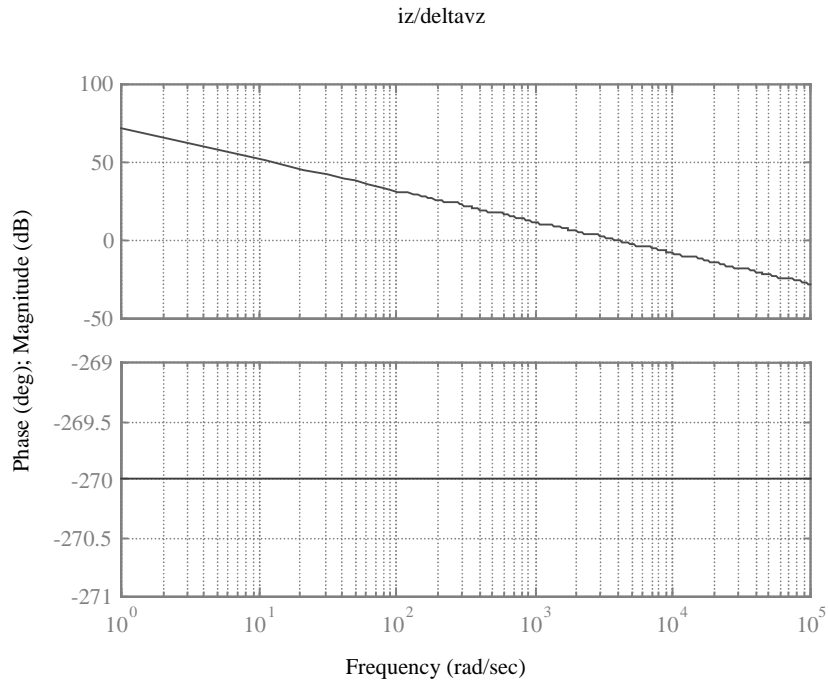


(b) $\tilde{i}_z / \tilde{d}_{q1}$.

Figure 3.27 Open-loop transfer functions of d- and q-channel control to z-channel current.



(a) $\tilde{i}_{p1} / \Delta \tilde{v}_z$.



(b) $\tilde{i}_z / \Delta \tilde{v}_z$.

Figure 3.28 Open-loop transfer functions of z-channel control to DC output and z-channel currents.

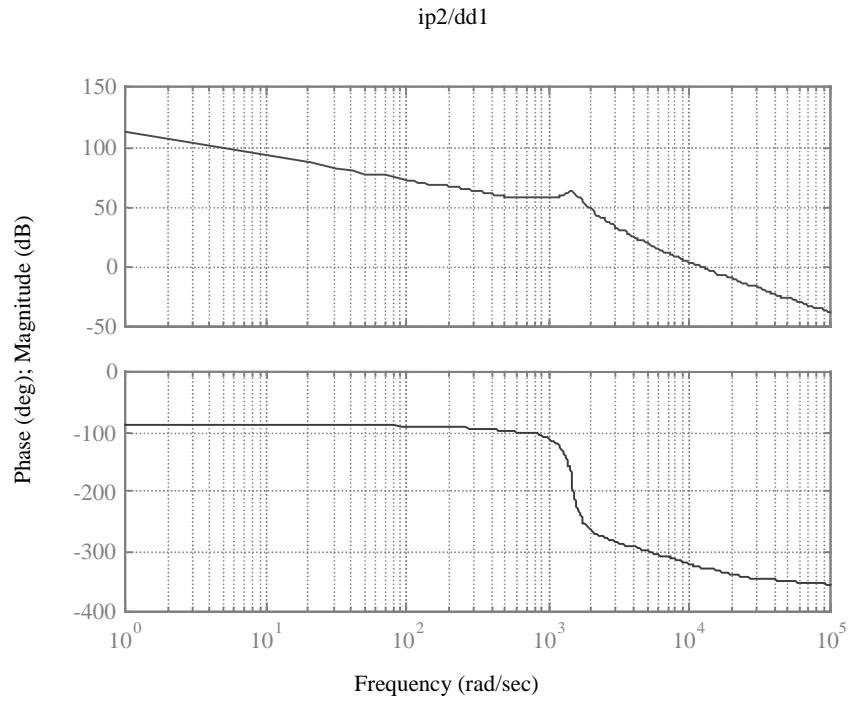


Figure 3.29 Open-loop transfer function $\tilde{i}_{p2} / \tilde{d}_{d1}$ shows the two converters are cross-coupled.

